Journal of Electron Microscopy **55(1)**: 23–26 (2006)
doi:dio: 10.1093/jmicro/dfl001

Physical: Note

Removing focused ion-beam damages on transmission electron microscopy specimens by using a plasma cleaner

Satoshi Hata[1,*], Harini Sosiati[2,3], Noriyuki Kuwano[3], Masaru Itakura[1], Takayoshi Nakano[4] and Yukichi Umakoshi[4]

[1]Department of Applied Science for Electronics and Materials, Kyushu University, Kasuga, Fukuoka 816-8580, Japan, [2]The Research Laboratory for High Voltage Electron Microscopy, Kyushu University, Fukuoka, Fukuoka 812-8581, Japan, [3]Art, Science and Technology Center for Cooperative Research, Kyushu University, Kasuga, Fukuoka 816-8580, Japan and [4]Division of Materials & Manufacturing Science, Graduate School of Engineering, Osaka University, Suita, Osaka 565-0871, Japan
*To whom correspondence should be addressed. E-mail: hata@asem.kyushu-u.ac.jp

Abstract A plasma cleaner is usually used for removing carbonaceous debris from a specimen and preventing contamination during transmission electron microscopy (TEM) imaging and analysis. However, the plasma cleaner can be effectively used for thinning down damage layers on TEM specimens prepared by focused ion-beam (FIB) milling. By optimizing plasma treatment conditions, the quality of high-resolution images and diffraction patterns of the FIB-milled specimens has been remarkably improved using the plasma cleaner.

Keywords focused ion beam, surface damage, plasma cleaner, transmission electron microscopy

Received 19 May 2005, accepted 26 January 2006, online 1 March 2006

Focused ion-beam (FIB) milling is a powerful method of specimen preparation for transmission electron microscopy (TEM). However, the FIB milling inherently produces damages on surfaces of TEM specimens. This phenomenon is generally explained as amorphization of the specimen surfaces by bombardment with accelerated Ga^+ ions. Since these damages degrade the quality of TEM images, a number of methods for removing the FIB damages were proposed: finishing with low-voltage FIB milling [1–3], subsequent treatments using an ion-beam mill [1,4,5] or a plasma cleaner [6–9], etc. There are advantages and disadvantages for each of these methods. For example, the low-voltage FIB milling can reduce thickness of the damage layer. However, changing the accelerating voltage during the operation is not convenient for some FIB mills. For an FIB-milled specimen prepared with a microsampling technique [2], the ion-beam milling needs some modifications in shapes of the microsample and a mesh for supporting the microsample. The plasma cleaner is usually used for removing carbonaceous debris from a specimen and preventing contamination during TEM imaging and analysis. Although preliminary applications of the plasma cleaner to the FIB damages have been reported by Bauer and co-workers [7–9], the effectiveness of using the plasma cleaner is still unclear, especially for high-resolution (HR) imaging.

In the present study, the plasma cleaner has been used for removing the FIB damages. HRTEM observations of three kinds of FIB-milled specimens have been carried out before and after the plasma treatment and effects of the plasma treatment on the FIB-milled specimens have been discussed.

A HITACHI FB-2000K FIB mill equipped with a microsampling system was used for specimen preparation. The accelerating voltage for the FIB milling was 30 kV, and final specimen thicknesses were less than 100 nm. A plasma cleaner, ULVAC PLASMA CUBE C50-MK (Fig. 1), equipped with a radio frequency (RF; 13.56 MHz) sputtering unit was used for plasma treatments after the FIB milling. An FIB-milled specimen was mounted on a TEM specimen holder and inserted into the chamber of the plasma cleaner. Argon plasma was produced in the chamber under the following conditions: the Ar gas pressure of 1.0–1.5 Pa, the RF power of 2–10 W and the plasma treatment time of 5–10 min. The voltage at the specimen during the plasma treatment was roughly estimated to be 100 V.

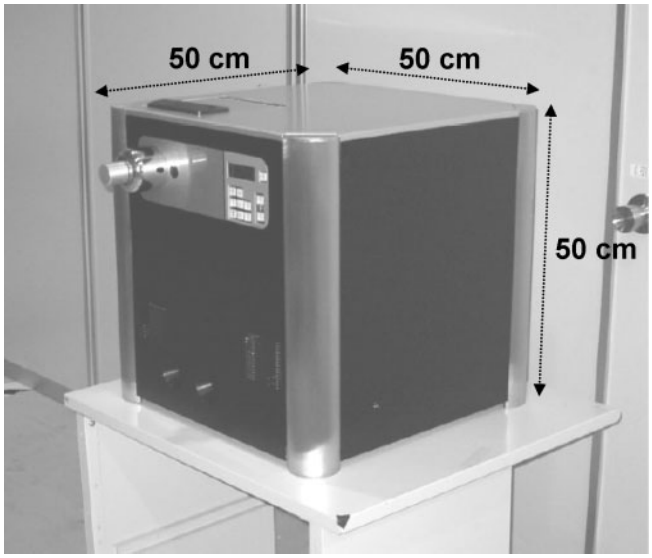

Fig. 1 A plasma cleaner (ULVAC PLASMA CUBE C50-MK) used in this work.

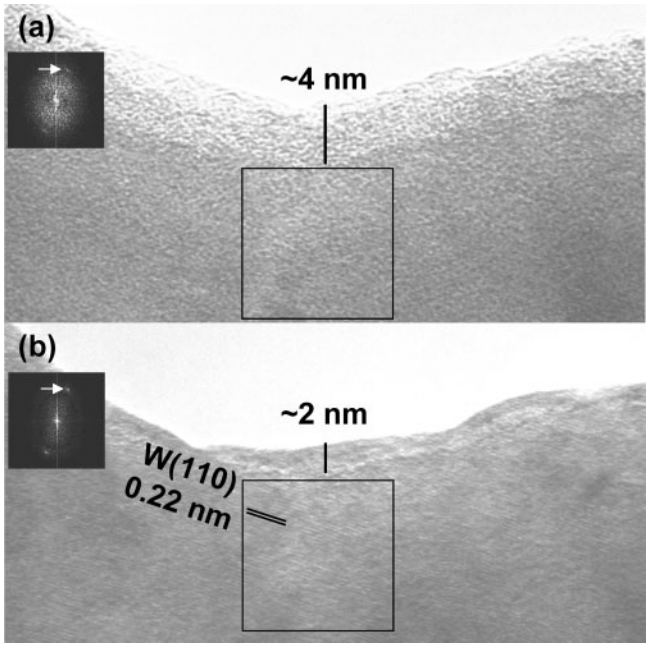

Fig. 2 Cross-sectional HRTEM images of a tungsten manipulator probe before (a) and after (b) the Ar plasma treatment at 5 W for 10 min. Fourier power spectra obtained from areas depicted with the open squares are inserted. Arrows in the spectra denote intensity maxima corresponding to lattice fringes from (110) planes of the tungsten crystal.

Figure 2a shows a cross-sectional HRTEM image of a tungsten manipulator probe used for the FIB microsampling process [2]. Although damaged zones at top and bottom surfaces of the specimen are not directly observed, an amorphous wall of 4 nm wide is recognized at the specimen edge. This suggests that the amorphous wall also exists at the top and bottom surfaces. The specimen was then exposed to the Ar plasma in the plasma cleaner. After the Ar plasma treatment at 5 W for 10 min, the width of the amorphous wall has reduced to ~2 nm, and lattice fringes corresponding to (110) planes of the tungsten crystals are visible, as shown in Fig. 2b. Figure 2 also shows Fourier power spectra obtained from square areas depicted with the open squares. Diffuse scattering around the direct beam is dominant in Fig. 2a, while a sharp intensity maximum at a position indicated by the arrow is clearly recognized in Fig. 2b. These features in the spectra confirm the reduction of the amorphous wall and the resultant improvement of the lattice fringe contrast after the plasma treatment.

Figure 3 shows cross-sectional HRTEM images of an yttria-stabilized zirconia (YSZ) film that is used as a substrate for an MgB_2 superconducting film [10–12]. For the as-FIB-milled specimen (Fig. 3a), lattice fringes of the YSZ crystals are observed in part of the observation area. After the Ar plasma treatment at 5 W for 10 min (Fig. 3b), the visibility of these lattice fringes has been slightly improved. Furthermore, after a subsequent plasma treatment at 2 W for 10 min (Fig. 3c), the visibility of the lattice fringes has been remarkably improved. The most significant effect of the plasma treatment at 2 W appears at thin areas near the specimen edge, as denoted with the open squares in Fig. 3. In Figs 3a and 3b, amorphous-like contrast is dominant. On the other hand, in Fig. 3c, lattice fringes corresponding to (200) planes of the YSZ crystal are visible at the same area. This appearance of the lattice fringes is confirmed with changes in the Fourier power spectra from the square areas, as indicated by the arrows in Fig. 3. It is interpreted for the YSZ specimen that the Ar plasma treatment at 5 W (Fig. 3b) creates additional damages as well as thinning down the FIB damages. Thus, setting the RF power at 2 W (Fig. 3c) is effective for suppressing the additional damages and reducing total thickness of the damage layer.

Figure 4 shows bright-field TEM images and diffraction patterns of an MgB_2/α-Al_2O_3 superconducting film [13–15], before (Fig. 4a) and after (Fig. 4b) an Ar plasma treatment at 10 W for 5 min. The image in Fig. 4a exhibits dark diffraction contrast due to fine columnar MgB_2 crystals 10–30 nm in size, and the visibility of this diffraction contrast is improved after the plasma treatment in Fig. 4b. At the same time, weak Bragg reflections from the MgB_2 crystals, indicated by the arrow in Fig. 4a, are clearly visible after the plasma treatment in Fig. 4b. These improvements in the images and diffraction patterns demonstrate the feasibility of the use of a plasma cleaner for removing FIB damages.

In summary, it is concluded that a plasma cleaner is quite useful for removing FIB damages on TEM specimens. Amorphous layers produced by the FIB milling are thinned down using the plasma cleaner, and the quality of TEM images and diffraction patterns are remarkably improved. Since the effectiveness of this method depends on the plasma treatment conditions such as the RF power, these conditions should be optimized for each material. For example, a low RF power (2 W or less) is preferable to avoid additional surface damages by the Ar plasma treatment. There can be

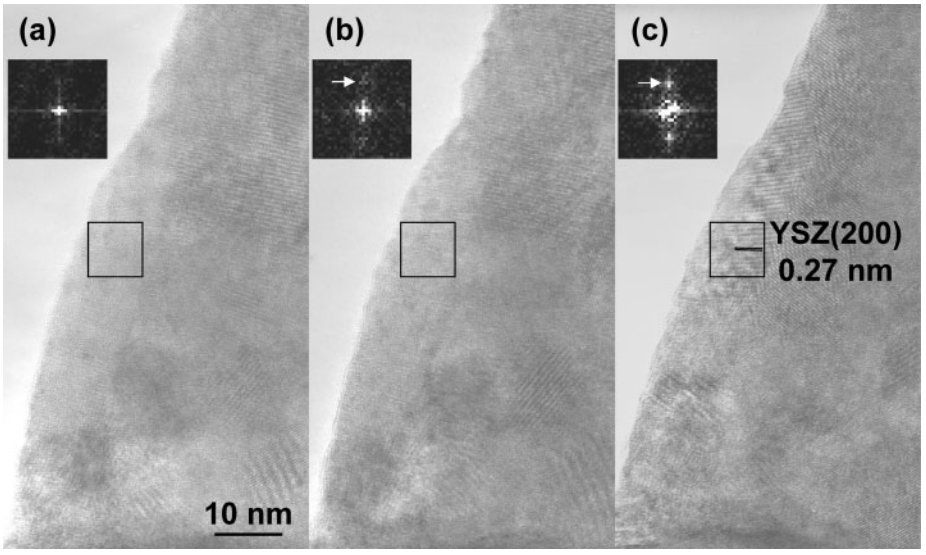

Fig. 3 Cross-sectional HRTEM images of a YSZ film. (a) As-FIB-milled specimen, (b) after the Ar plasma treatment at 5 W for 10 min, (c) after the subsequent treatment at 2 W for 10 min. Fourier power spectra obtained from areas depicted with the open squares are inserted. Arrows in the spectra denote intensity maxima corresponding to lattice fringes from (200) planes of the YSZ crystal.

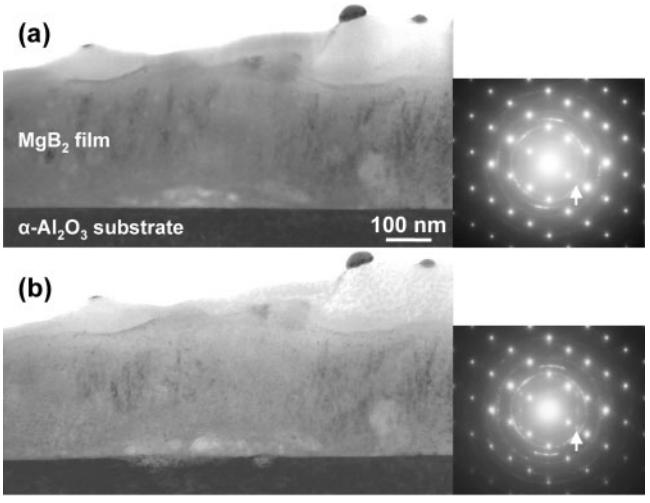

Fig. 4 Cross-sectional bright-field TEM images and diffraction patterns of an MgB_2/α-Al_2O_3 film. (a) As-FIB-milled specimen and (b) after the Ar plasma treatment at 10 W for 5 min. Arrows in the diffraction patterns denote Bragg reflections from the MgB_2 crystals.

some attempts for developing this method: use of different gas (Ar + O_2, etc.), effects of the plasma treatment on electron energy loss spectroscopy measurements, etc. Since TEM specimen holders are commonly used for most of the commercial plasma cleaners, these attempts can be easily performed by repeating the plasma treatment and subsequent TEM imaging and analysis.

Acknowledgements

The authors thank Y. Mineno (ULVAC), S. Miyazaki (FEI) and B. Arnold (IFW Dresden) for their valuable comments. This work was partly supported by Industrial Technology Research Program (Project: 03A47002) in 2003 from New Energy and Industrial Technology Development Organization (NEDO) of Japan. This work was supported in part by Nanotechnology Support Project of the Ministry of Education, Culture, Sports, Science and Technology (MEXT), Japan.

References

1 Kato N I (2004) Reducing focused ion beam damage to transmission electron microscopy samples. *J. Electron Microsc.* **53:** 451–458.

2 Kamino T, Yaguchi T, Kuroda Y, Ohnishi T, Ishitani T, Miyahara Y, and Horita Z (2004) Evaluation of TEM samples of an Mg–Al alloy prepared using FIB milling at the operating voltages of 10 kV, 40 kV. *J. Electron Microsc.* **53:** 459–463.

3 Yabuuchi Y, Tametou S, Okano T, Inazato S, Sadayama S, Yamamoto Y, Iwasaki K, and Sugiyama Y (2004) A study of the damage on FIB-prepared TEM samples of $Al_xGa_{1-x}As$. *J. Electron Microsc.* **53:** 471–477.

4 McCaffrey J P, Phaneuf M W, and Madsen L D (2001) Surface damage formation during ion-beam thinning of samples for transmission electron microscopy. *Ultramicroscopy* **87:** 97–104.

5 Sasaki H, Matsuda T, Kato T, Muroga T, Iijima Y, Saitoh T, Iwase F, Yamada Y, Izumi T, Shiohara Y, and Hirayama T (2004) Specimen preparation for high-resolution transmission electron microscopy using focused ion beam, Ar ion milling. *J. Electron Microsc.* **53:** 497–500.

6 South Bay Technology Inc. (2002), South Bay Technology, Inc., CA, USAPlasma Trimming™. *In: Model PC2000 Plasma Cleaner Catalogue*. South Bay Technology, Inc., CA, USA.

7 Bauer H-D, Arnold B, and Binder K (2002) Avoiding, removing of undesired surface damages on FIB prepared TEM specimens. In Cross R, and Richards P (2002) (eds), *Proceedings of the ICEM 15* S32, CD1, (The Microscopy Society of Southern Africa).

8 Arnold B, Lohse D, Bauer H-D, Gemming T, Wetzig K, and Binder K (2003) Surface damages on FIB prepared TEM-specimens: possibilities of avoidance, removal. *Microsc. Microanal.* **9** (Suppl.)**:** 140–141.

9 Arnold B, and Bauer H-D (2003) Experiences in cross section preparation of layered materials by FIB-method. *Prakt. Metallogr.* **40:** 109–130.

10 Sosiati H, Hata S, Kuwano N, Tomokiyo Y, Matsumoto A, Fukutomi M, Kitaguchi H, Komori K, and Kumakura H (2004) Electron microscopy of MgB_2 thin film on YSZ-buffered Hastelloy. *Physica C* **412–414:** 1376–1382.

11 Hata S, Sosiati H, Kuwano N, Tomokiyo Y, Matsumoto A, Fukutomi M, Kitaguchi H, Komori K, and Kumakura H (2005) Effects of heat treatments on microstructure formation in MgB_2/YSZ/Hastelloy film. *IEEE Trans. Appl. Supercond.* **15:** 3238–3241.

12 Hata S, Sosiati H, Tomokiyo Y, Kuwano N, Matsumoto A, Fukutomi M, Kitaguchi H, Komori K, and Kumakura H (2005) Microstructure of MgB_2 films deposited on YSZ/Hastelloy substrate. *J. Japan Inst. Metals* **68:** 648–655.

13 Kitaguchi H, Matsumoto A, Kumakura H, Doi T, Yamamoto H, Saitoh K, Sosiati H, and Hata S (2004) MgB_2 films with very high critical current densities due to strong grain boundary pinning. *Appl. Phys. Lett.* **85:** 2842–2844.

14 Sosiati H, Hata S, Kuwano N, Tomokiyo Y, Kitaguchi H, Doi T, Yamamoto H, Matsumoto A, Saitoh K, and Kumakura H (2005) Relationship between microstructure, J_c property in MgB_2/α-Al_2O_3 film fabricated by *in situ* electron beam evaporation. *Supercond. Sci. Technol.* **18:** 1275–1279.

15 Kitaguchi H, Doi T, Kobayashi Y, Matsumoto A, Sosiati H, Hata S, Fukutomi M, and Kumakura H (2005) Properties of MgB_2 films with very high transport critical current densities. *IEEE Trans. Appl. Supercond.* **15:** 3313–3316.